Available online at www.sciencedirect.com
ScienceDirect
Progress in Natural Science 19 (2009) 313–320
Progress in Natural Science
www.elsevier.com/locate/pnsc

Guided elastic waves in infinite free-clamped hollow cylinders

Liguo Tang [a,b,*], Shengxing Liu [a,b]

[a] Department of Oceanography, Xiamen University, Xiamen 361005, China
[b] Key Laboratory of Underwater Acoustic Communication and Marine Information Technology of the Ministry of Education, Xiamen University, Xiamen 361005, China

Received 19 May 2008; received in revised form 20 June 2008; accepted 25 June 2008

Abstract

Guided elastic-wave-inspection technique for hollow cylinders has received plenty of attention in recent years because of its high efficiency and low cost. To apply guided elastic waves to defects detection, it is necessary to investigate the propagation of guided waves in the hollow cylinders under all kinds of boundary conditions. In this paper, the dispersion equations of torsional, longitudinal and flexural guided waves in the hollow cylinders with traction-free and clamped lateral boundaries are derived by elastodynamic theory, based on which the phase and group velocity dispersion curves of the guided waves mentioned above are obtained. And the dispersion properties of these waves are discussed in detail. The transient wave in a free-clamped hollow cylinder is simulated by the finite element method (FEM). The time–frequency distribution of the transient wave agrees well with the theoretical group velocity dispersion curves.

Keywords: Guided elastic waves; Free-clamped hollow cylinders; Dispersion

1. Introduction

The pioneering work of Silk and Bainton [1] on the use of guided waves for the inspection of heat exchanger tubing made people notice the potential value of this technique. It offers the possibility of rapid nondestructive evaluation of long lengths of pipework for corrosion and cracks. It is necessary to investigate the propagation of guided waves in the hollow cylinders under all kinds of boundary conditions in order to employ them to detect the defects mentioned above. The propagation of guided waves in the infinite hollow cylinders with traction-free lateral boundaries has been studied intensively by Gazis [2]. According to his studies, various guided wave modes propagating axially in the hollow cylinders can be categorized as torsional waves $T(0,m)$, longitudinal waves $L(0,m)$ and flexural waves $F(n,m)$ $(n,\ m=1,2,3,\ldots)$. There are also guided waves propagating circumferentially. The excitation of transient guided waves in the infinite hollow cylinders has been investigated by Ditri and Rose [3], Pan et al. [4], and Tang and Cheng [5]. Han et al. [6] studied the transient waves in a cylinder made of functionally graded material by a hybrid numerical method. As to the free vibrations of the finite length hollow cylinders with traction-free lateral boundaries, Hutchinson and EI-Azhari [7], and Mofakhami et al. [8] presented a semi-analytical method, in which some of the boundary conditions need to be approximately satisfied using the orthogonalization technique while the others need to be exact. Aristegui et al. [9], Na and Kundu [10], and Pan et al. [11] investigated the propagation of guided waves in fluid-filled tubes.

There are few published papers about the propagation of guided waves in the hollow cylinders with traction-free and clamped lateral boundaries, i.e. one lateral boundary is clamped while the other is traction free. Bird [12] discussed the plane-strain vibration of these hollow

* Corresponding author. Tel.: +86 13696992450; fax: +86 592 2186397.
E-mail address: liguotang@xmu.edu.cn (L. Tang).

1002-0071/$ - see front matter © 2008 National Natural Science Foundation of China and Chinese Academy of Sciences. Published by Elsevier Limited and Science in China Press. All rights reserved.
doi:10.1016/j.pnsc.2008.06.015

cylinders numerically. In this paper, the propagation of torsional waves, longitudinal waves and flexural waves in the hollow cylinders with traction-free and clamped lateral boundaries is investigated theoretically and numerically. Note that an infinite hollow cylinder is called free clamped, when its inside surface is free and its outside surface is clamped; contrarily, it is called clamped free in the sequel.

2. Dispersion properties of guided waves

The free vibration of an isotropic elastic solid is governed by Navier's equation

$$(\lambda+\mu)\nabla(\nabla\cdot\boldsymbol{u})+\mu\nabla^2\boldsymbol{u}=\rho\frac{\partial^2\boldsymbol{u}}{\partial t^2} \tag{1}$$

where λ and μ are the Lamé constants of the material, and $\boldsymbol{u}(\boldsymbol{r},t)$ is the displacement field vector. According to the method of Helmholtz resolution [13], we have

$$\boldsymbol{u}=\boldsymbol{L}+\boldsymbol{M}+\boldsymbol{N} \tag{2}$$

$$\boldsymbol{L}=\nabla\varphi,\quad \boldsymbol{M}=\nabla\times(\psi\boldsymbol{e}_z),\quad \boldsymbol{N}=l\nabla\times\nabla\times(\chi\boldsymbol{e}_z) \tag{3}$$

where l is introduced so that these terms are dimensionally uniform, $\boldsymbol{e}_z$ is the unit vector along the axial coordinate directions. φ, ψ and χ in Eq. (3), which are called the Helmholtz potentials, satisfy

$$\nabla^2\varphi+\frac{\omega^2}{c_1^2}\varphi=0 \tag{4}$$

$$\nabla^2\psi+\frac{\omega^2}{c_2^2}\psi=0 \tag{5}$$

$$\nabla^2\chi+\frac{\omega^2}{c_2^2}\chi=0 \tag{6}$$

where $c_1=\sqrt{(\lambda+2\mu)/\rho}$ and $c_2=\sqrt{\mu/\rho}$. We can obtain the following expressions of displacement and stress components from Eqs. (2)–(6):

$$u_r(r,\theta,z,t)=R_r(r)\cos n\theta\cos\xi z e^{j(\xi z-\omega t)} \tag{7}$$

$$u_\theta(r,\theta,z,t)=R_\theta(r)\sin n\theta\cos\xi z e^{j(\xi z-\omega t)} \tag{8}$$

$$u_z(r,\theta,z,t)=R_z(r)\cos n\theta\sin\xi z e^{j(\xi z-\omega t)} \tag{9}$$

$$\sigma_{rr}(r,\theta,z,t)=\tau_{rr}(r)\cos n\theta\cos\xi z e^{j(\xi z-\omega t)} \tag{10}$$

$$\sigma_{r\theta}(r,\theta,z,t)=\tau_{r\theta}(r)\sin n\theta\cos\xi z e^{j(\xi z-\omega t)} \tag{11}$$

$$\sigma_{rz}(r,\theta,z,t)=\tau_{rz}(r)\cos n\theta\sin\xi z e^{j(\xi z-\omega t)} \tag{12}$$

where

$$\begin{bmatrix}R_r(r)\\R_\theta(r)\\R_z(r)\\\tau_{rr}(r)\\\tau_{r\theta}(r)\\\tau_{rz}(r)\end{bmatrix}=\begin{bmatrix}S_{11}&S_{12}&\cdots&S_{16}\\S_{21}&S_{22}&\cdots&S_{26}\\S_{31}&S_{32}&\cdots&S_{36}\\T_{11}&T_{12}&\cdots&T_{16}\\T_{21}&T_{22}&\cdots&T_{26}\\T_{31}&T_{32}&\cdots&T_{36}\end{bmatrix}\cdot\begin{bmatrix}A_1\\B_1\\A_2\\B_2\\A_3\\B_3\end{bmatrix} \tag{13}$$

The expressions of S_{ij} and T_{ij} $(i=1,2,3;\ j=1,2,\ldots,6)$ are listed in Appendix A.

For a free-clamped hollow cylinder, i.e. the inside surface of the hollow cylinder is traction free and the outside surface of it is clamped, we have

$$\sigma_{rr}|_{r=a}=0,\quad \sigma_{r\theta}|_{r=a}=0,\quad \sigma_{rz}|_{r=a}=0 \tag{14}$$

$$u_r|_{r=b}=0,\quad u_\theta|_{r=b}=0,\quad u_z|_{r=b}=0 \tag{15}$$

where a and b are the inner and outer radiuses, respectively. For a clamped-free hollow cylinder, i.e. the inside surface of the hollow cylinder is clamped and the outside surface of it is traction free, we have

$$u_r|_{r=a}=0,\quad u_\theta|_{r=a}=0,\quad u_z|_{r=a}=0 \tag{16}$$

$$\sigma_{rr}|_{r=b}=0,\quad \sigma_{r\theta}|_{r=b}=0,\quad \sigma_{rz}|_{r=b}=0 \tag{17}$$

Fig. 1 is the schematic diagram of the infinite hollow cylinder with free and clamped lateral boundaries.

Substituting Eqs. (7)–(12) in Eqs. (14) and (15) or Eqs. (16) and (17), we obtain a system of six homogeneous equations in the constants A_1, B_1, A_2, B_2, A_3 and B_3. A necessary and sufficient condition for the existence of a solution is that the determinant of coefficients must be equal to zero, namely,

$$|C_{pq}|_{6\times6}=0 \tag{18}$$

where

$$C_{pq}=\begin{cases}T_{pq}\big|_{r=a} & (p=1,2,3;\ q=1,2,\cdots6)\\ S_{(p-3)q}\big|_{r=b} & (p=4,5,6;\ q=1,2,\cdots6)\end{cases} \tag{19}$$

for the free-clamped hollow cylinder, and

$$C_{pq}=\begin{cases}S_{pq}\big|_{r=a} & (p=1,2,3;\ q=1,2,\cdots6)\\ T_{(p-3)q}\big|_{r=b} & (p=4,5,6;\ q=1,2,\cdots6)\end{cases} \tag{20}$$

for the clamped-free hollow cylinder. If $n\neq0$, Eq. (18) represents the dispersion equation of flexural waves. If $n=0$, we can derive from Eq. (18) that

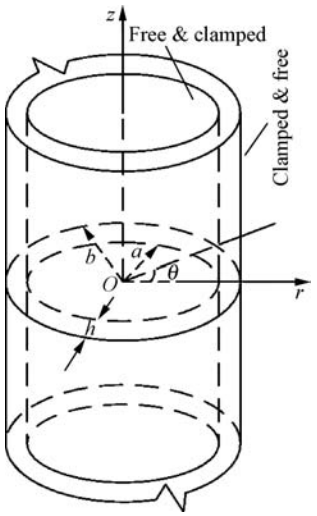

Fig. 1. Schematic diagram of an infinite hollow cylinder with free and clamped lateral boundaries.

$$\begin{vmatrix} C_{11} & C_{12} & 0 & 0 & C_{15} & C_{16} \\ 0 & 0 & C_{23} & C_{24} & 0 & 0 \\ C_{31} & C_{32} & 0 & 0 & C_{35} & C_{36} \\ C_{41} & C_{42} & 0 & 0 & C_{45} & C_{46} \\ 0 & 0 & C_{53} & C_{54} & 0 & 0 \\ C_{61} & C_{62} & 0 & 0 & C_{65} & C_{66} \end{vmatrix} = 0 \tag{21}$$

Eq. (21) yields

$$\begin{vmatrix} C_{23} & C_{24} \\ C_{53} & C_{54} \end{vmatrix} = 0 \tag{22}$$

and

$$\begin{vmatrix} C_{11} & C_{12} & C_{15} & C_{16} \\ C_{31} & C_{32} & C_{35} & C_{36} \\ C_{41} & C_{42} & C_{45} & C_{46} \\ C_{61} & C_{62} & C_{65} & C_{66} \end{vmatrix} = 0 \tag{23}$$

Eqs. (22) and (23) are the dispersion equations of torsional and longitudinal waves, respectively.

Numerical results show that the guided waves in the clamped-free hollow cylinder almost propagate in the same manner as those in the free-clamped one. Thus, only the numerical results for the guided waves propagating in the free-clamped hollow cylinder are given here. The material parameters employed in all simulations are density $\rho = 7.8\ \mathrm{g/cm^3}$, Young's module $E = 215.04\ \mathrm{GPa}$, and the Poisson coefficient $\gamma = 0.28$.

The dispersion equation of guided waves in the hollow cylinder can be expressed as

$$f(c, \xi) = 0 \tag{24}$$

where c is the phase velocity, and ξ is the wave number. For a fixed value of ξ, the left part of Eq. (24) is a function of c alone. Muller and bisection methods can be used to find the roots of it. Compared with the Muller method, the bisection method is less efficient but more robust. Here, we use the latter one. Note that some adjacent phase velocity dispersion curves of longitudinal or flexural guided waves are very close in the vicinity of some points. It may greatly lower the efficiency of root finding, because the step size Δc must be very small when some roots are very close to each other. In order to improve the efficiency of computation, the algorithm of variable step size Δc is adopted. The roots $c_i\,(i = 1, 2, \ldots, k)$ found at the given value of ξ are stored, and the intervals $\Delta c_i\,(i = 1, 2, \ldots, k-1)$ between the roots are computed, where k is the number of roots we want to compute. When we search for the roots at $\xi + \Delta\xi$, the step size Δc changes according to the location of c and Δc_i.

Fig. 2 shows the Phase and Group velocity (C_p and C_g) dispersion curves of the torsional waves $T(0, m)$, longitudinal waves $L(0, m)$ and flexural waves $F(1, m)$ in the free-clamped hollow cylinder with $h/b = 0.1$, where $m = 1, 2, \ldots, 10$ and h is the wall thickness. The dispersion curves corresponding to the guided waves in free-free hollow cylinders, whose inside and outside surfaces are traction free, are shown in Fig. 3.

The guided waves in the free-clamped hollow cylinder have the following properties:

(1) Fig. 2(a) and (b) shows that all the torsional wave modes in the free-clamped hollow cylinder are dispersive. But the mode $T(0, 1)$ in the free–free hollow cylinder is nondispersive (as shown in Fig. 3(a) and (b)).
(2) We can find from Fig. 2(d) that the mode $L(0, 1)$ in the free-clamped hollow cylinder has the cut-off frequency. And Fig. 2(c) shows that the phase velocity of this mode is greater than c_2, when $\xi h < 3.0$. But the mode $L(0, 1)$ in the free–free hollow cylinder has no cut-off frequency, i.e. the energy of it is distributed in the frequency band of $[0, \infty)$, which can be known from Fig. 3(c) and (d), and the phase velocity of it is less than c_2 when $\xi h \ni (0.2, 3)$.
(3) By comparing Fig. 2(d) and (e) with Fig. 3(d) and (e), we can observe that the group velocity dispersion curves of the guided waves in the free-clamped hollow cylinder are more complex than those in the free–free one.
(4) The phase velocity of the mode $F(1, 1)$ in the free-clamped hollow cylinder is greater than c_2 when ξh is small enough, as shown in Fig. 2(e). But Fig. 3(e) shows that the phase velocity of the mode $F(1, 1)$ in the free–free hollow cylinder is always less than c_2.
(5) Fig. 2(d) and (f) shows that the modes $L(0, 2)$, $L(0, 4)$, $F(1, 3)$ and $F(1, 6)$ in the free-clamped hollow cylinder contain frequency components with negative group velocity. Fig. 3(d) and (f) shows that the modes $L(0, 4)$ and $F(1, 6)$ contain but $L(0, 2)$ and $F(1, 3)$ do not contain frequency components with negative group velocity for the free–free hollow cylinder. By comparing Fig. 2(d) and (f) with Fig. 3(d) and (f), we can find that the maximal absolute value of the negative group velocity of the mode $L(0, 4)$ or $F(1, 6)$ in the free-clamped hollow cylinder is smaller than that of the corresponding mode in the free–free one.
(6) By comparing Fig. 2(b), (d) and (f) with Fig. 3(b), (d) and (f), we know that the cut-off frequency of the guided wave mode in the free-clamped hollow cylinder is different from that of the corresponding mode in the free–free one.
(7) It seems from Fig. 2(c) and (e) that some adjacent phase velocity dispersion curves of longitudinal or flexural guided waves intersect each other, for example, those of $L(0, 1)$ and $L(0, 2)$ or $F(1, 1)$ and $F(1, 2)$. But this is not the truth. Fig. 4(a)–(c) shows the phase velocity dispersion curves of the guided wave modes $F(1, m)$ $(m = 1, 2, \ldots, 10)$ in the free-clamped hollow cylinders with different h/b. It is easy to observe from Fig. 4(a) that the adjacent phase velocity dispersion curves do not intersect each other when h/b is big enough, but they begin to attract each other at some points when h/b decreases gradually, as shown in Fig. 4(b) and (c). And they are so close that they seem

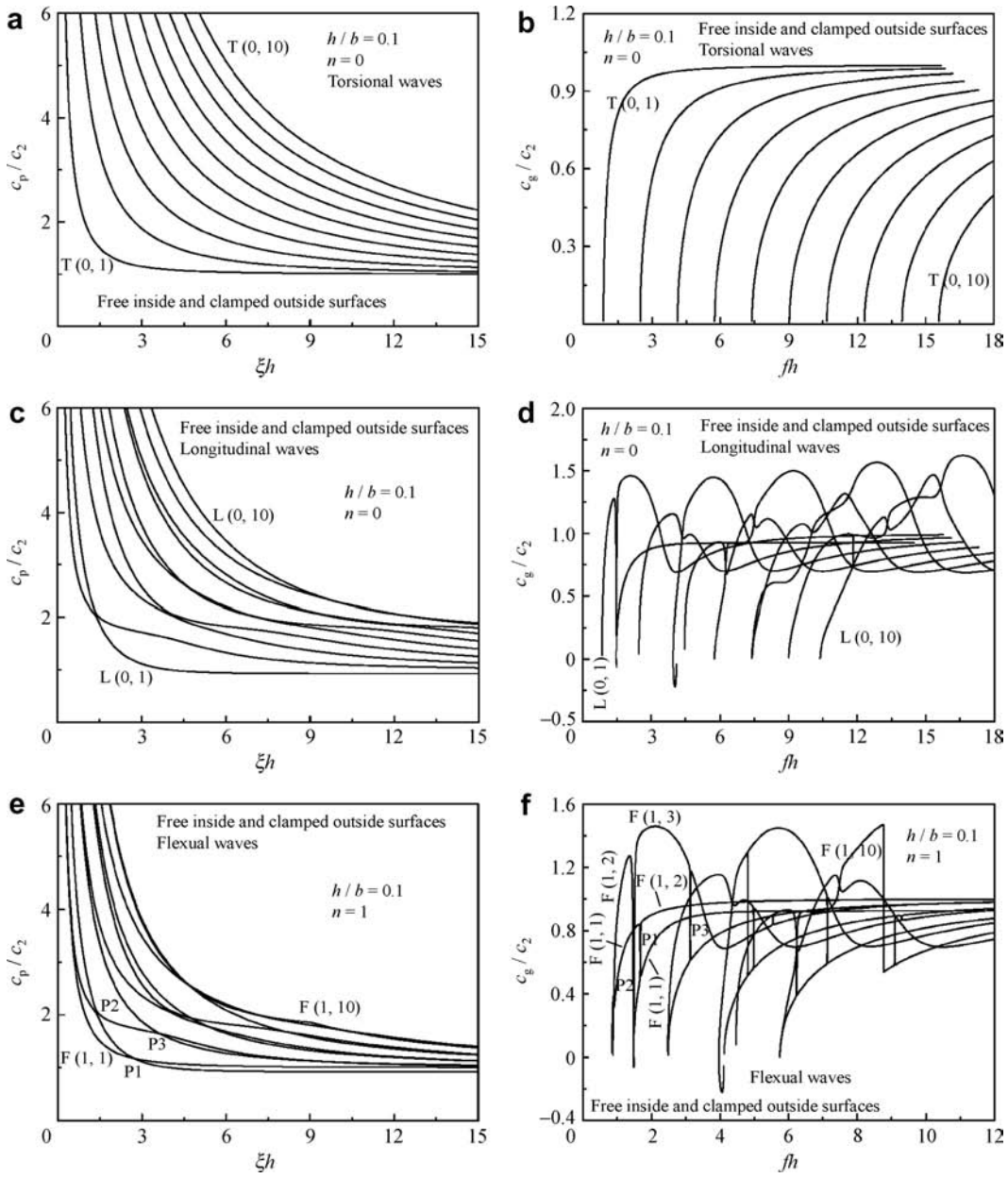

Fig. 2. The dispersion curves of guided waves in the free-clamped hollow cylinder with $h/b = 0.1$. (a) Phase velocity dispersion curves of torsional waves $T(0,m)$; (b) group velocity dispersion curves of torsional waves $T(0,m)$; (c) phase velocity dispersion curves of longitudinal waves $L(0,m)$; (d) group velocity dispersion curves of longitudinal waves $L(0,m)$; (e) phase velocity dispersion curves of flexural waves $F(1,m)$; (f) group velocity dispersion curves of flexural waves $F(1,m)$ in the free-clamped hollow cylinder with $h/b = 0.1$, where $m = 1,2,\ldots,10$.

to intersect each other when h/b is small enough. Fig. 2(e) shows that the phase velocity dispersion curves of modes $F(1,1)$ and $F(1,2)$, $F(1,2)$ and $F(1,3)$, and $F(1,3)$ and $F(1,4)$ attract each other at points P1, P2 and P3, respectively. Fig. 2(f) shows that the group velocity dispersion curves corresponding to these points vary sharply.

3. Transient waves and analyses

In this section, we will investigate the propagation of transient waves in the free-clamped steel hollow cylinder, the geometrical parameters of which are outer radius $b = 0.04$ m and wall thickness $h = 0.01$ m, by the finite element method (FEM). The external force is applied on the inside surface axisymmetrically along the radial direction, and it is formulated as

$$S(z,t) = A\left[e^{-0.1\varepsilon(t-\kappa)^2} - e^{-0.1\varepsilon(t-1.1\kappa)^2} + 2e^{-5\varepsilon(t-\kappa)^2} - 2e^{-5\varepsilon(t-1.1\kappa)^2}\right]\boldsymbol{e}_r, \quad z \in [-L,L],\ \theta \in [0,2\pi] \tag{25}$$

where

$$\varepsilon = 10^{12}, \quad \kappa = 10^{-5}, \quad L = 0.5 \times 10^{-3} m \tag{26}$$

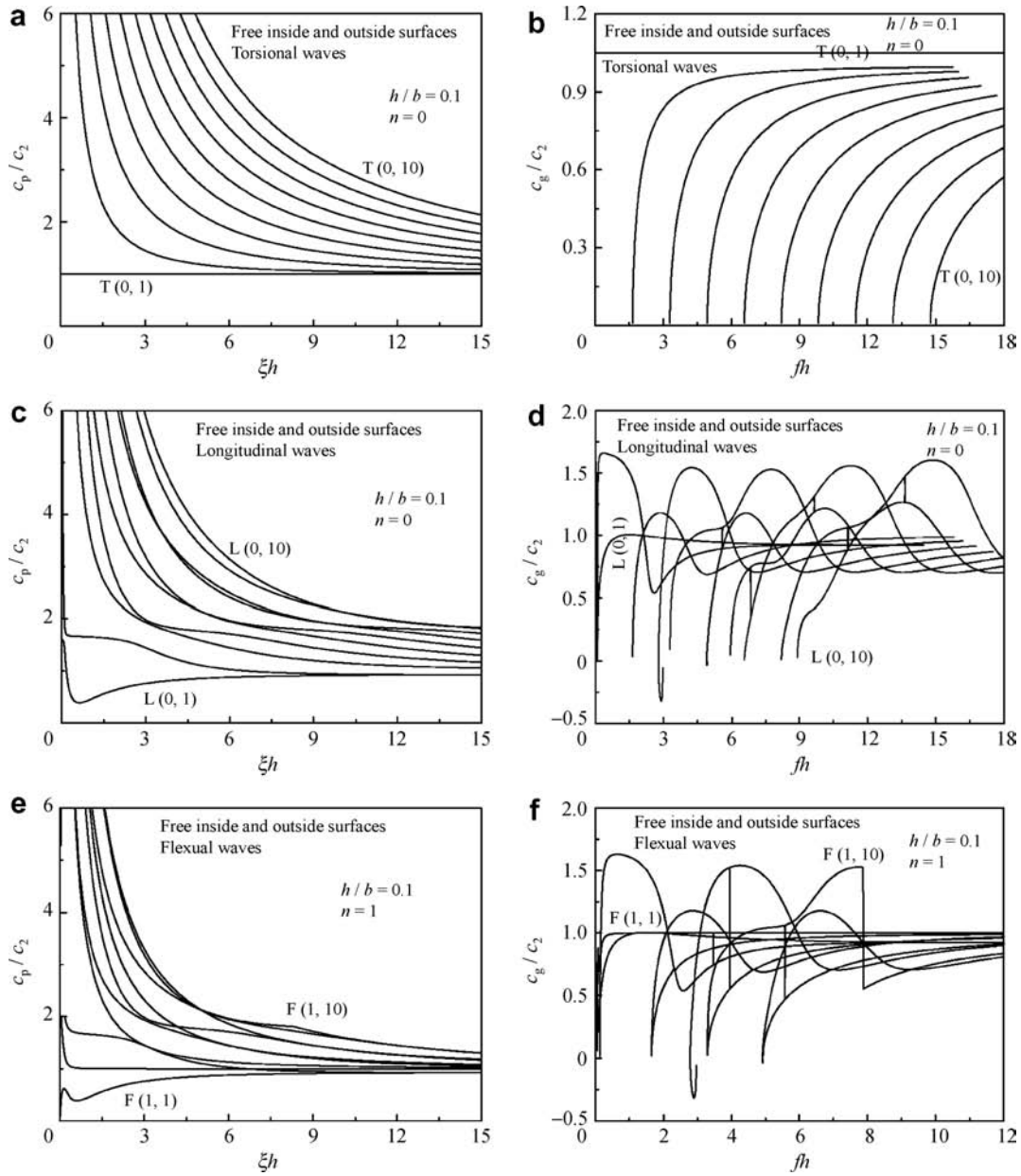

Fig. 3. The dispersion curves of guided waves in the free–free hollow cylinder with $h/b = 0.1$. (a) Phase velocity dispersion curves of torsional waves $T(0,m)$; (b) group velocity dispersion curves of torsional waves $T(0,m)$; (c) phase velocity dispersion curves of longitudinal waves $L(0,m)$; (d) group velocity dispersion curves of longitudinal waves $L(0,m)$; (e) phase velocity dispersion curves of flexural waves $F(1,m)$; (f) group velocity dispersion curves of flexural waves $F(1,m)$ in the free–free hollow cylinder with $h/b = 0.1$, where $m = 1,2,\ldots,10$.

Fig. 5(a) is the normalized waveform of $\boldsymbol{S}(a,z,t)$, and Fig. 5(b) is the normalized power spectrum density (PSD) of it. Apparently, only the longitudinal wave modes can be excited. Simulation indicates that the excitation efficiency of the mode $L(0,1)$ is far higher than that of the other mode, especially in the neighborhood of 200 kHz, if the exciting source is an impact signal whose energy is distributed in a wide frequency range. Thus, the external force formulated as in Eqs. (25) and (26) is constructed to adjust the distribution of energy in different wave modes to make it easy to analyze the dispersion properties of different modes from the transient waves excited. We can find from Fig. 5(b) that the energy of the source is relatively low in the neighborhood of 200 kHz.

Fig. 6 shows the finite element mesh of the hollow cylinder. The finite element model can be reduced, because the hollow cylinder and the surface force applied to it are not only axis-symmetrical but also symmetric to the plane $z = 0$. Four-noded two-dimensional axisymmetric elements are employed in the FEM simulation. The element size along the z-axis is 2.5×10^{-4} m. And the hollow cylinder is radially divided into forty uniform parts. The time-step is 0.025 μs in the explicit algorithm. And the following

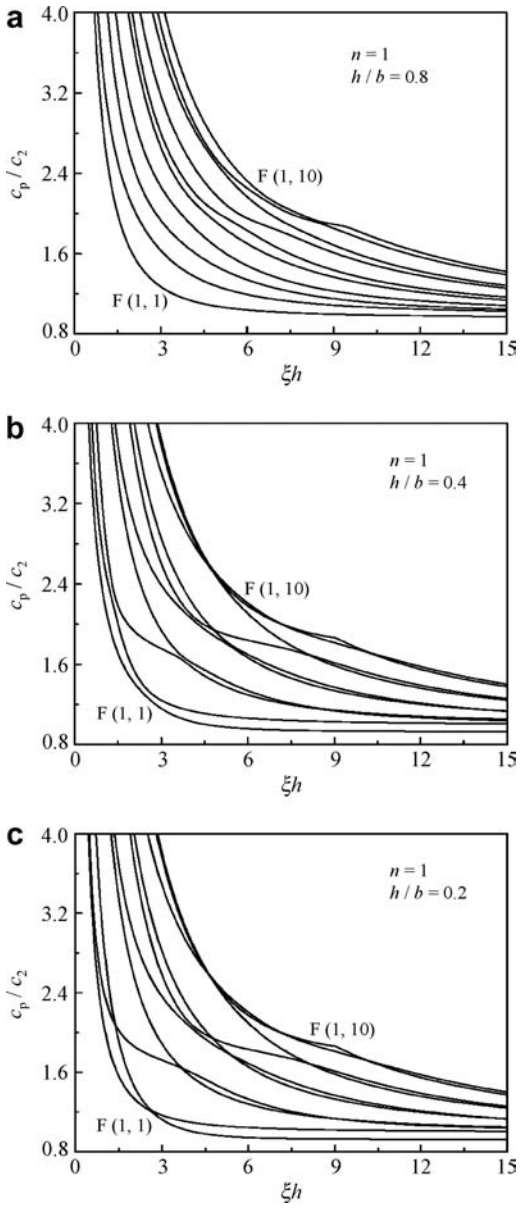

Fig. 4. The phase velocity dispersion curves of the guided wave modes $F(1,m)$ $(m = 1, 2, \ldots, 10)$ in the free-clamped hollow cylinders with different h/b. (a) $h/b = 0.8$; (b) $h/b = 0.4$; (c) $h/b = 0.2$.

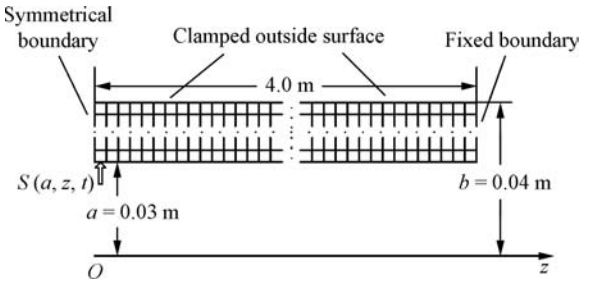

Fig. 6. The finite element mesh of the hollow cylinder employed in the FEM simulation.

results are obtained by employing the general purpose commercial finite element software called Abaqus.

Fig. 7(a)–(c) shows the transient axial displacement u_z simulated by FEM at $z = 1.0$ m, 1.5 m and 2.0 m, respectively. Clearly, the amplitude of the transient displacement becomes smaller and the waveform expands along

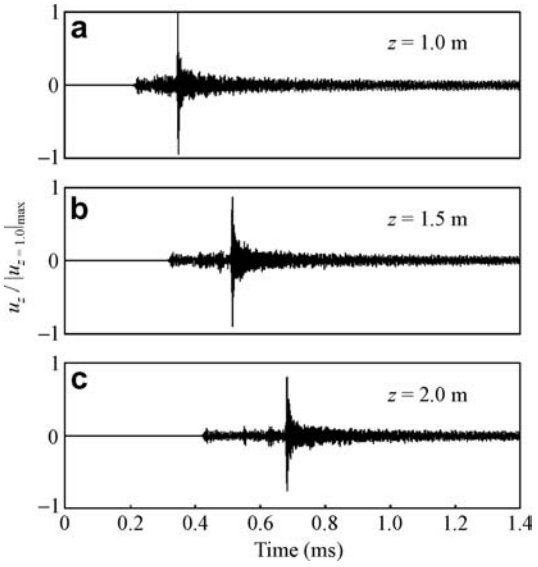

Fig. 7. The transient axial displacement u_z simulated by FEM. (a) $z = 1.0$ m; (b) $z = 1.5$ m; (c) $z = 2.0$ m.

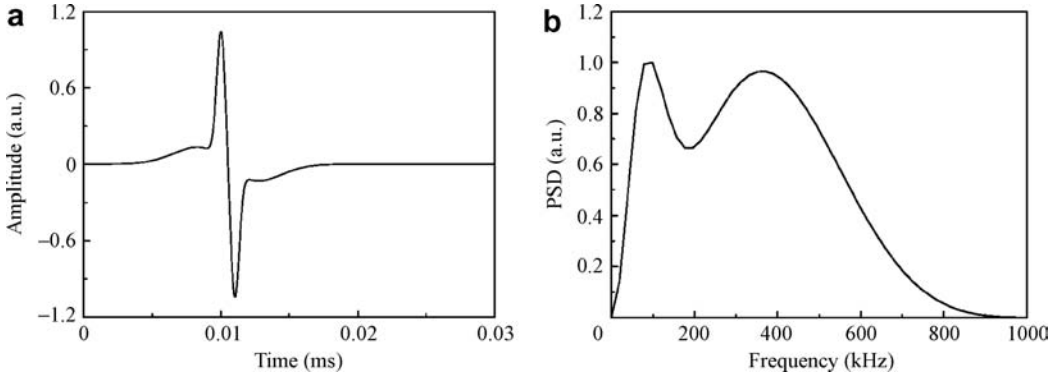

Fig. 5. The normalized waveform of $\boldsymbol{S}(a,z,t)$ (a) and the normalized power spectrum density (PSD) of the source $\boldsymbol{S}(a,z,t)$ (b).

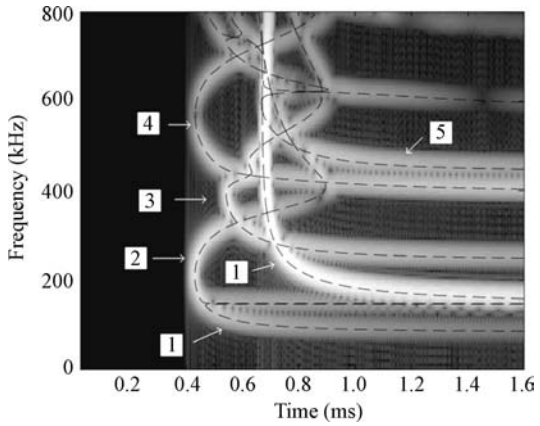

Fig. 8. The time–frequency distribution of the wave in Fig. 7(c).

with the propagation of the guided waves because of the dispersion effect. Fig. 8 shows the time–frequency distribution of the wave in Fig. 7(c). The time–frequency distribution gives the arrival time of each frequency component and, therefore, directly shows the relationship between the group velocity and the frequency. We can conclude from Fig. 8 that the sharp spikes with high amplitude in Fig. 7 come from higher frequency of the mode $L(0,1)$ propagating at a relatively unvarying group velocity. The dash line in Fig. 8 is the group velocity dispersion curves computed from the dispersion equation, i.e. Eq. (23). Apparently, they agree very well with the time–frequency distribution of the transient waveform simulated by FEM.

4. Conclusions

Generally, a single pure mode needs to be excited, and then employed to detect the defects in elastic guides in order to extract useful information from the waves reflected from the defects easily; otherwise, the waves caused by the interaction of multimodes and the defects may be too complex to be analyzed. Studying the dispersion properties of the guided waves is the basis of selecting the approximate mode to inspect the hollow cylinder [14], which is the motivation of this study. The dispersion properties of the guided waves in the free-clamped hollow cylinder have been discussed theoretically and numerically in this study. To prove the correctness of the theoretical and numerical results, the time–frequency distribution of the transient wave simulated by FEM is obtained and is compared with the theoretical dispersion results. Good agreement is obtained.

Acknowledgement

This work was supported by the National Natural Science Foundation of China (Grant No. 10704064).

Appendix A

The expressions of S_{ij} and T_{ij} ($i = 1,2,3$; $j = 1,2,\ldots,6$) in Eq. (13) are

$$S_{11} = \alpha_1 Z_n'(\alpha_1 r) \tag{A1}$$
$$S_{12} = \alpha_1 W_n'(\alpha_1 r) \tag{A2}$$
$$S_{13} = \frac{n}{r} Z_n(\beta_1 r) \tag{A3}$$
$$S_{14} = \frac{n}{r} W_n(\beta_1 r) \tag{A4}$$
$$S_{15} = j\xi\beta_1 l Z_n'(\beta_1 r) \tag{A5}$$
$$S_{16} = j\xi\beta_1 l W_n'(\beta_1 r) \tag{A6}$$
$$S_{21} = -\frac{n}{r} Z_n(\alpha_1 r) \tag{A7}$$
$$S_{22} = -\frac{n}{r} W_n(\alpha_1 r) \tag{A8}$$
$$S_{23} = -\beta_1 Z_n'(\beta_1 r) \tag{A9}$$
$$S_{24} = -\beta_1 W_n'(\beta_1 r) \tag{A10}$$
$$S_{25} = -\frac{jn\xi l}{r} Z_n(\beta_1 r) \tag{A11}$$
$$S_{26} = -\frac{jn\xi l}{r} W_n(\beta_1 r) \tag{A12}$$
$$S_{31} = -j\xi Z_n(\alpha_1 r) \tag{A13}$$
$$S_{32} = -j\xi W_n(\alpha_1 r) \tag{A14}$$
$$S_{33} = 0 \tag{A15}$$
$$S_{34} = 0 \tag{A16}$$
$$S_{35} = l\left(\frac{\omega^2}{c_2^2} - \xi^2\right) Z_n(\beta_1 r) \tag{A17}$$
$$S_{36} = l\left(\frac{\omega^2}{c_2^2} - \xi^2\right) W_n(\beta_1 r) \tag{A18}$$
$$T_{11} = 2\mu\alpha_1^2 Z_n''(\alpha_1 r) - \lambda \cdot \frac{\omega^2}{c_1^2} \cdot Z(\alpha_1 r) \tag{A19}$$
$$T_{12} = 2\mu\alpha_1^2 W_n''(\alpha_1 r) - \lambda \cdot \frac{\omega^2}{c_1^2} \cdot W_n(\alpha_1 r) \tag{A20}$$
$$T_{13} = 2\mu \frac{n}{r^2} [\beta_1 r Z_n'(\beta_1 r) - Z_n(\beta_1 r)] \tag{A21}$$
$$T_{14} = 2\mu \frac{n}{r^2} [\beta_1 r W_n'(\beta_1 r) - W_n(\beta_1 r)] \tag{A22}$$
$$T_{15} = 2j\mu\xi\beta_1^2 l Z_n''(\beta_1 r) \tag{A23}$$
$$T_{16} = 2j\mu\xi\beta_1^2 l Z_n''(\beta_1 r) \tag{A24}$$
$$T_{21} = -\frac{2\mu n\alpha_1}{r} Z_n'(\alpha_1 r) + \frac{2\mu n}{r^2} Z_n(\alpha_1 r) \tag{A25}$$
$$T_{22} = -\frac{2\mu n\alpha_1}{r} W_n'(\alpha_1 r) + \frac{2\mu n}{r^2} W_n(\alpha_1 r) \tag{A26}$$
$$T_{23} = \frac{\mu n^2}{r^2} Z_n(\beta_1 r) + \frac{\mu\beta_1}{r} Z_n'(\beta_1 r) - \mu\beta_1^2 Z_n''(\beta_1 r) \tag{A27}$$
$$T_{24} = \frac{\mu n^2}{r^2} W_n(\beta_1 r) + \frac{\mu\beta_1}{r} W_n'(\beta_1 r) - \mu\beta_1^2 W_n''(\beta_1 r) \tag{A28}$$
$$T_{25} = -\frac{2j\mu n\xi\beta_1 l}{r} Z_n'(\beta_1 r) + \frac{2j\mu n\xi l}{r^2} Z_n(\beta_1 r) \tag{A29}$$

$$T_{26} = -\frac{2j\mu n\xi\beta_1 l}{r} W'_n(\beta_1 r) + \frac{2j\mu n\xi l}{r^2} W_n(\beta_1 r) \tag{A30}$$

$$T_{31} = 2j\mu\xi\alpha_1 Z'_n(\alpha_1 r) \tag{A31}$$

$$T_{32} = 2j\mu\xi\alpha_1 W'_n(\alpha_1 r) \tag{A32}$$

$$T_{33} = j\frac{\mu n\xi}{r} Z_n(\beta_1 r) \tag{A33}$$

$$T_{34} = j\frac{\mu n\xi}{r} W_n(\beta_1 r) \tag{A34}$$

$$T_{35} = \mu l\beta_1 \left[\frac{\omega^2}{c_2^2} - 2\xi^2\right] Z'_n(\beta_1 r) \tag{A35}$$

$$T_{36} = \mu l\beta_1 \left[\frac{\omega^2}{c_2^2} - 2\xi^2\right] W'_n(\beta_1 r) \tag{A36}$$

where

$$\alpha_1^2 = \lambda_1\alpha^2, \quad \beta_1^2 = \lambda_2\beta^2 \tag{A37}$$

$$\alpha^2 = \frac{\omega^2}{c_1^2} - \xi^2, \quad \beta^2 = \frac{\omega^2}{c_2^2} - \xi^2 \tag{A38}$$

$$\lambda_1 = \begin{cases} 1, & \alpha^2 > 0 \\ -1, & \alpha^2 < 0 \end{cases}, \quad \lambda_2 = \begin{cases} 1, & \beta^2 > 0 \\ -1, & \beta^2 < 0 \end{cases} \tag{A39}$$

References

[1] Silk MG, Bainton KF. The propagation in metal tubing of ultrasonic wave modes equivalent to Lamb waves. Ultrasonics 1979;17:11–9.

[2] Gazis DC. Three-dimensional investigation of the propagation of waves in hollow circular cylinders: I. Analytical foundation. J Acoust Soc Am 1959;31:568–73.

[3] Ditri JJ, Rose JL. Excitation of guided elastic wave modes in hollow cylinders by applied surface tractions. J Appl Phys 1992;72:2589–97.

[4] Pan Y, Li L, Rossignol C, et al. Acoustic waves generated by a laser line pulse in a hollow cylinder. Ultrasonics 2006;44:843–7.

[5] Tang LG, Cheng JC. Numerical analysis on laser-generated guided elastic waves in a hollow cylinder. J Nondestruct Eval 2002;21:45–53.

[6] Han X, Liu GR, Xi ZC, et al. Transient waves in a functionally graded cylinder. Int J Solids Struct 1999;38:3021–37.

[7] Hutchinson JR, EI-Azhari SA. Vibrations of free hollow circular cylinders. J Appl Mech 1986;53:641–6.

[8] Mofakhami MR, Toudeshky HH, Hashemi SH. Finite cylinder vibrations with different end boundary conditions. J Sound Vib 2006;297:293–314.

[9] Aristegui C, Lowe MJS, Cawley P. Guided waves in fluid-filled pipes surrounded by different fluids. Ultrasonics 2001;39:367–75.

[10] Na WB, Kundu T. Underwater pipeline inspection using guided waves. J Press Vess 2002;124:196–200.

[11] Pan HT, Koyano K, Usui Y. Experimental and numerical investigations of axisymmetric wave propagation in cylindrical pipe filled with fluid. J Acoust Soc Am 2003;113:3209–14.

[12] Bird JF, Hare RW, McClure FT. Vibrations of thick-walled hollow cylinders: exact numerical solutions. J Acoust Soc Am 1960;32:1404–12.

[13] Eringen AC, Suhubi ES. Elastodynamics. New York: Academic Press; 1975, p. 718–23.

[14] Alleyne DN, Lowe M, Cawley P. The excitation of Lamb waves in pipes using dry coupled piezoelectric transducers. J Nondestruct Eval 1996;15:1–20.